

Synthesis, in vitro and in vivo biological evaluation of novel graveolinine derivatives as potential anti-Alzheimer agents

Wen Luo, Jian-Wu Lv, Ting Wang, Zhi-Yang Zhang, Hui-Yan Guo, Zhi-Yi Song, Chao-Jie Wang, Jing Ma, Yi-ping Chen

PII: S0968-0896(19)31182-4  
DOI: <https://doi.org/10.1016/j.bmc.2019.115190>  
Reference: BMC 115190

To appear in: *Bioorganic & Medicinal Chemistry*

Received Date: 11 July 2019  
Revised Date: 28 October 2019  
Accepted Date: 29 October 2019

Please cite this article as: W. Luo, J-W. Lv, T. Wang, Z-Y. Zhang, H-Y. Guo, Z-Y. Song, C-J. Wang, J. Ma, Y-p. Chen, Synthesis, in vitro and in vivo biological evaluation of novel graveolinine derivatives as potential anti-Alzheimer agents, *Bioorganic & Medicinal Chemistry* (2019), doi: <https://doi.org/10.1016/j.bmc.2019.115190>

This is a PDF file of an article that has undergone enhancements after acceptance, such as the addition of a cover page and metadata, and formatting for readability, but it is not yet the definitive version of record. This version will undergo additional copyediting, typesetting and review before it is published in its final form, but we are providing this version to give early visibility of the article. Please note that, during the production process, errors may be discovered which could affect the content, and all legal disclaimers that apply to the journal pertain.



## Synthesis, in vitro and in vivo biological evaluation of novel graveolinine derivatives as potential anti-Alzheimer agents

Wen Luo <sup>§,a</sup>, Jian-Wu Lv <sup>§,a</sup>, Ting Wang <sup>a</sup>, Zhi-Yang Zhang <sup>a</sup>, Hui-Yan Guo <sup>a</sup>, Zhi-Yi Song <sup>b</sup>, Chao-Jie Wang <sup>a</sup>, Jing Ma <sup>b,\*</sup>, Yi-ping Chen <sup>c,\*</sup>

<sup>a</sup> *Key Laboratory of Natural Medicine and Immuno-Engineering, Henan University, Kaifeng 475004, People's Republic of China*

<sup>b</sup> *Institute for Innovative Drug Design and Evaluation, Henan University, Kaifeng 475004, People's Republic of China*

<sup>c</sup> *School of Pharmaceutical Sciences, Guangxi University of Chinese Medicine, Nanning 530001, People's Republic of China*

\* Jing Ma: Email [majing.1988.ok@163.com](mailto:majing.1988.ok@163.com), Tel 086 0371-23880680, Fax 086 0371-23880680

\* Yi-ping Chen: Email [yipchen2009@foxmail.com](mailto:yipchen2009@foxmail.com), Tel 086 0771-4733943, Fax 086 0771-4953042

§ The first two authors contributed equally to this work.

### ABSTRACT

A novel series of graveolinine derivatives were synthesized and evaluated as potential anti-Alzheimer agents. Compound **5f** exhibited the best inhibitory activity for acetylcholinesterase (AChE) and had surprisingly potent inhibitory activity for butyrylcholinesterase (BuChE), with IC<sub>50</sub> values of 0.72 μM and 0.16 μM, respectively. The results from Lineweaver–Burk plot and molecular modeling study

indicated non-competitive inhibition of AChE by compound **5f**. In addition, these derivatives showed potent self-induced  $\beta$ -amyloid ( $A\beta$ ) aggregation inhibition. Moreover, **5f** didn't show obvious toxicity against PC12 and HepG2 cells at 50  $\mu$ M. Finally, *in vivo* studies confirmed that **5f** significantly ameliorates the cognitive performances of scopolamine-treated ICR mice. Therefore, these graveolinine derivatives should be thoroughly and systematically studied for the treatment of Alzheimer's disease.

## KEYWORDS

Graveolinine

Acetylcholinesterase

Butyrylcholinesterase

$\beta$ -amyloid

Alzheimer's disease

## 1. Introduction

Alzheimer's disease (AD) is one of the most common diseases in elderly people and is characterized by irreversible neuronal damage that causes dementia, cognitive impairment, and memory loss [1]. The observation of a deficiency in cholinergic neurotransmission in AD led to the cholinergic hypothesis [2]. According to the hypothesis, the current mainstays of AD treatment have focused on acetylcholinesterase (AChE) inhibitors aimed at increasing acetylcholine (ACh) levels in the brain [3]. Acetylcholinesterase inhibitors represent a well-established class of drugs for the symptomatic treatment of AD, which include donepezil, rivastigmine, galantamine and huperzine A. Among them, galantamine and huperzine A are naturally-occurring alkaloids from the genus *Galanthus* (Amaryllidaceae) and the club moss *Huperzia serrata* (Lycopodiaceae), respectively.

Two major cholinesterases (ChEs), AChE and butyrylcholinesterase (BuChE), are involved in the hydrolysis and regulation of ACh in vertebrates [4]. Various cholinergic drugs, especially AChE inhibitors also function as BuChE inhibitors. Moreover, the use of agents with enhanced selectivity for BuChE, including MF-8622 and cymserine indicated the potential therapeutic benefit of inhibiting BuChE in AD and related dementias [5]. BuChE specific inhibition is unlikely to be associated with adverse events and may show efficacy without remarkable side effects [6]. Therefore, BuChE may be considered as an important target for novel drug development to treat AD. In the future, the development of specific BuChE inhibitors and the continued use of ChEs inhibitors may lead to improved clinical outcomes [7].

Graveolinine (Fig. 1) belongs to the 2-phenyl quinolone compounds, alkaloids isolated from *Ruta graveolens* L. (Common Rue Herb) in the south of China [8]. It is an isomer of graveoline which is also an alkaloid from ethanolic extract of *Ruta graveolens*. Graveolinine can be converted to graveoline

in DMF/MeI at 80 °C [9]. Although a few of studies have reported its antibacterial, spasmolytic and anti-tumor activities [10-12], studies regarding the synthesis and biological activity of graveolinine derivatives are rare, especially there are almost no reports about the anti-AD activities of graveolinine and its derivatives. Although in 2016, there was a report by Li et al about the synthesis and AChE inhibitory activity of graveoline analogs [13], actually, these analogs don't belong to graveolinine derivatives.

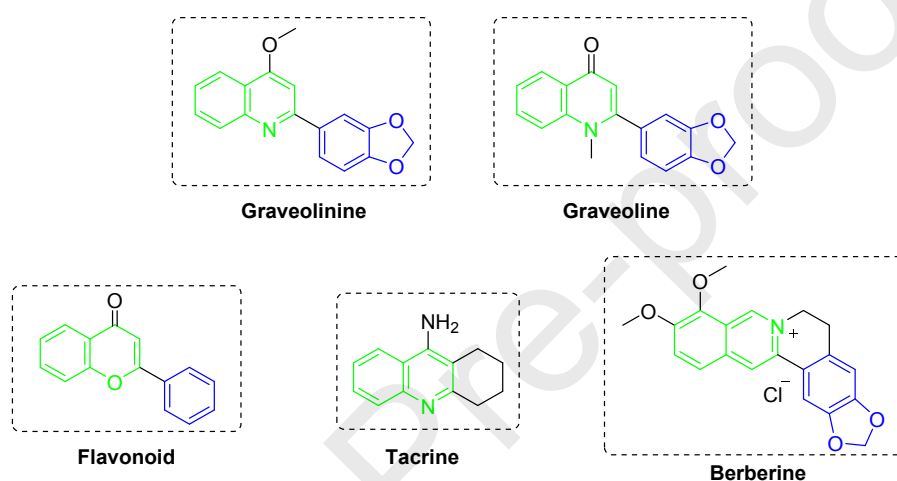


**Figure 1.** Chemical structures of graveolinine, graveoline, flavonoid, tacrine and berberine.

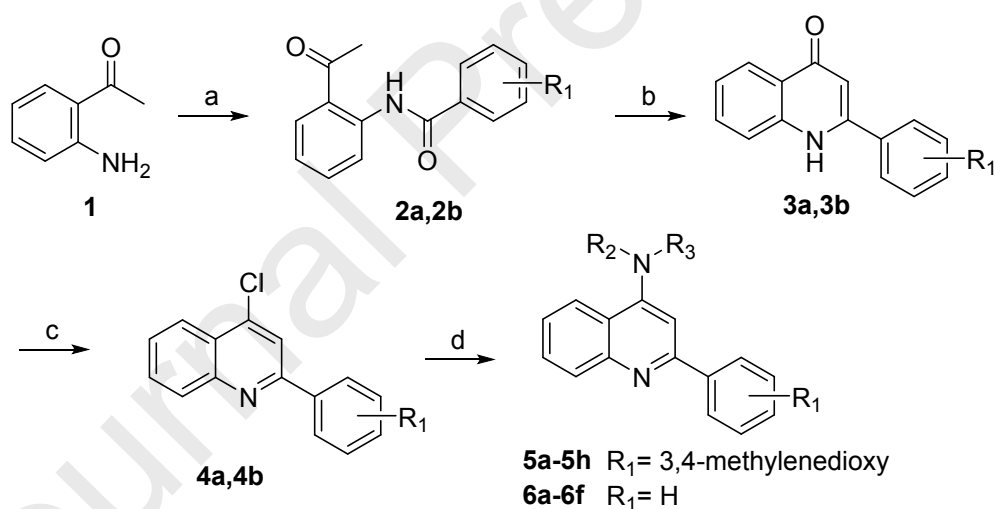
Our group has focused on the development of ChEs inhibitors as anti-AD agents for many years. We have previously studied flavonoids and their derivatives as ChEs inhibitors and found that these derivatives showed moderate inhibitory potency, but lacked good solubility and contained too many flexible rotation bonds [14-16]. Therefore, we are now focused on the development of more potent ChEs inhibitors isolated or derived from natural products. Our search indicated graveolinine might be of interest because its structure is similar to that of flavonoids, two aromatic rings connected by one rotating bond, and to tacrine (Fig. 1), which contains a quinolone ring. Moreover, the structure of graveolinine is also similar with berberine, which contains a dioxymethylene group, showed significant inhibitory activities for both ChEs (IC<sub>50</sub> value: 0.37 μM for *ee*AChE, 18.2 μM for *eq*BuChE)

and  $\beta$ -amyloid ( $A\beta$ ) aggregation [17-18].

Based on these similar structure features, a series of graveolinine derivatives with 4-methoxyl group modified on the quinolone ring were designed and synthesized. To explore the structure-activity relationship, some compounds lacking dioxymethylene were also synthesized. These were then evaluated for their biological activity, including *in vitro* ChEs and  $A\beta$  aggregation inhibitory activities, cytotoxicity towards human hepatoma cell line HepG2 and rat pheochromocytoma cell line PC12. The *in vivo* pro-cognitive effects of **5f** were also evaluated through the application of scopolamine in mice and exposing to Morris water maze (MWM).

## 2. Results and discussion

### 2.1. Chemistry



**Scheme 1.** Synthesis of graveolinine derivatives. Reagents and conditions: (a) piperonyl chloride or benzoyl chloride,  $\text{CH}_2\text{Cl}_2$ ,  $\text{Et}_3\text{N}$ , r.t. 24 h; (b)  $(\text{CH}_3)_3\text{COK}$ ,  $(\text{CH}_3)_3\text{COH}$ ,  $75^\circ\text{C}$ , 16 h; (c)  $\text{POCl}_3$ , reflux, 4 h; (d) amines,  $\text{K}_2\text{CO}_3$ ,  $135^\circ\text{C}$ , 4 h.

The synthetic route for the graveolinine derivatives starting from commercially available 1-(2-aminophenyl) ethanone (**1**) was outlined in Scheme 1. Condensation of starting material (**1**) with piperonyl chloride or benzoyl chloride in the presence of  $\text{Et}_3\text{N}$  in  $\text{CH}_2\text{Cl}_2$  at room temperature

produced **2a** and **2b**. The ketone (**2a** or **2b**) was treated with strong base  $(\text{CH}_3)_3\text{COK}$  to obtain intermediates (**3a** or **3b**) in satisfactory yield. The chlorination of **3a** or **3b** with  $\text{POCl}_3$  provided **4a** or **4b** in good yields. Finally, the reaction of **4a** or **4b** with different amines produced the targets compounds **5a-5h** and **6a-6f** in 51-83% yields. All the compounds were characterized by  $^1\text{H}$  NMR,  $^{13}\text{C}$  NMR and MS.

## 2.2. Inhibition studies on AChE and BuChE

The AChE and BuChE inhibition effects of the target compounds were determined using the spectroscopic method described by Ellman et al [19]. Rivastigmine, a well-known cholinesterase inhibitor, was used as the positive control. The precursor compound graveoline was also evaluated for comparative purpose. The results are listed in Table 1, expressed as  $\text{IC}_{50}$  values.

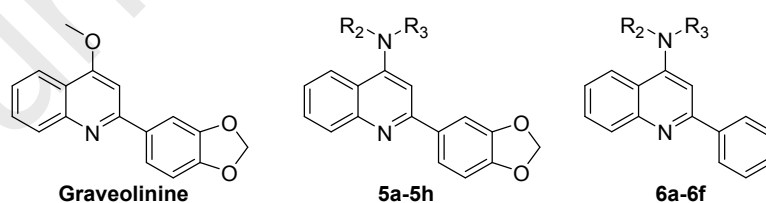
Almost all the tested target compounds showed moderate inhibitory activity for both AChE and BuChE. The precursor compound graveoline presented weak ChEs inhibitory potency. Interestingly, compound **5f** possessed a noteworthy BuChE inhibitory activity with  $\text{IC}_{50}$  of 0.16  $\mu\text{M}$ . The results showed that introduction of the pyrrolidine group at the 4-position increased the ChEs inhibitory capacity and improved the selectivity for BuChE over AChE. The selective BuChE inhibitors may provide therapeutic advantages in patients with advanced stages of AD. Because in AD, the AChE level in the brain decreases progressively, but BuChE activity remains the same or increases up to 165% of the normal level. As shown in Table 1, the structure of terminal group of side chain significantly affected the inhibitory activities for BuChE. The potencies to inhibit BuChE were in the order **5d**, **6d** (piperidine substituted) > **5e**, **6e** (morpholine substituted) > **5a**, **6a** (hydroxyl substituted). The screening data also showed that the methylene chain length had significant effects on BuChE inhibitory activities, the order of potencies is **5c**, **6c** (6 methylenes) > **5b**, **6b** (4 methylenes) > **5a**, **6a** (3

methylenes).

For AChE inhibition, the precursor compound graveolinine did not show potent inhibitory activity, but introduction of the substituent group ( $\text{NR}_2\text{R}_3$ ) increased the AChE inhibitory capacity. The results revealed that variation of the substituted group had a smaller influence on their inhibition of AChE compared with BuChE. Compounds **5f** and **6f**, containing a pyrrolidine group, exhibited the best inhibitory activity for AChE, with  $\text{IC}_{50}$  values of 0.72  $\mu\text{M}$  and 3.71  $\mu\text{M}$ , respectively.

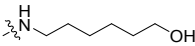
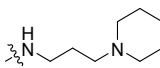
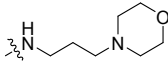
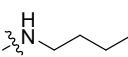
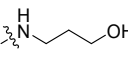
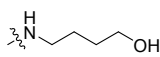
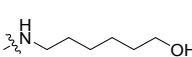
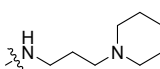
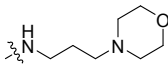
Compounds with the same substituted group (such as **5a** and **6a**), but different mother nucleus were compared. Compounds containing a graveolinine nucleus (**5a-5f**) had a greater AChE inhibitory activity compared with compounds containing a 2-phenyl quinolone nucleus (**6a-6f**). This indicated that dioxymethylene is a significant for AChE inhibition activity.

In addition, compounds **5f** and **5g** attracted our interest, when the pyrrolidine of compound **5f** was replaced with an piperidine group to form compound **5g**, the resulting inhibition activity for both ChEs was decreased about 10-fold compared with **5f**. This finding might be explained by an increase in steric hindrance of the piperidine group, which would prevent compound **5g** to interact optimally with the residues in the binding site of ChEs.



**Table 1.** Inhibition of ChEs activity and selectivity index of the target compounds

Compds.	$\text{NR}_2\text{R}_3$	$\text{IC}_{50}^{\text{a}}$ for AChE ( $\mu\text{M}$ )	$\text{IC}_{50}^{\text{b}}$ for BuChE ( $\mu\text{M}$ )	$\text{SI}^{\text{c}}$	$\text{A}\beta$ inhibition (%) <sup>d</sup>
<b>5a</b>		4.23±0.20	>10	<0.42	36.61±1.79
<b>5b</b>		4.26±0.12	9.78±0.28	0.44	44.13±3.71

<b>5c</b>		4.32±0.07	6.49±0.33	0.67	39.37±5.68
<b>5d</b>		4.78±0.13	1.45±0.08	3.3	65.59±4.29
<b>5e</b>		3.22±0.17	8.15±0.39	0.40	61.64±4.63
<b>5f</b>		0.72±0.06	0.16±0.01	4.5	62.52±2.93
<b>5g</b>		>10	2.09±0.12	>4.8	48.55±2.38
<b>5h</b>		4.80±0.21	7.85±0.12	0.61	30.63±2.56
<b>6a</b>		>10	>10	-	36.80±0.84
<b>6b</b>		9.85±1.35	4.31±0.16	2.3	40.71±1.61
<b>6c</b>		6.22±0.37	2.96±0.11	2.1	29.16±3.18
<b>6d</b>		>10	1.19±0.09	>8.4	60.31±5.10
<b>6e</b>		>10	4.44±0.21	>2.3	55.51±2.44
<b>6f</b>		3.71±0.24	0.43±0.05	8.6	57.68±3.87
Graveolinine	-	36.3±1.40	28.2±0.84	1.3	26.92±3.33
Rivastigmine	-	6.35±1.50	1.51±0.09	4.2	-
Curcumin	-	-	-	-	52.26±3.30

<sup>a</sup> AChE from *electric eel*; <sup>b</sup> BuChE from *equine serum*; <sup>c</sup> Selectivity Index = IC<sub>50</sub> (AChE) / IC<sub>50</sub> (BuChE); <sup>d</sup> The thioflavin-T (ThT) fluorescence method was used and the compounds were used at a concentration of 20 μM. Data are represented as mean ± SD.

### 2.3 Kinetic characterization of AChE inhibition

We cultured the crystal of **5f** with *Torpedo californica* AChE to elucidate the interaction patterns of **5f** with AChE; though, no positive results were obtained. The mechanism of inhibition of AChE was investigated using the derivative **5f**, the most potent AChE inhibitor. Steady state inhibition data of compound **5f** for AChE is shown in Figure 2. Lineweaver-Burk reciprocal plots revealed an increasing

slope and an increasing intercept at higher inhibitor concentrations, and the four lines intersected at the x-axis. This pattern indicates a non-competitive inhibition which is similar with that of berberine [20].

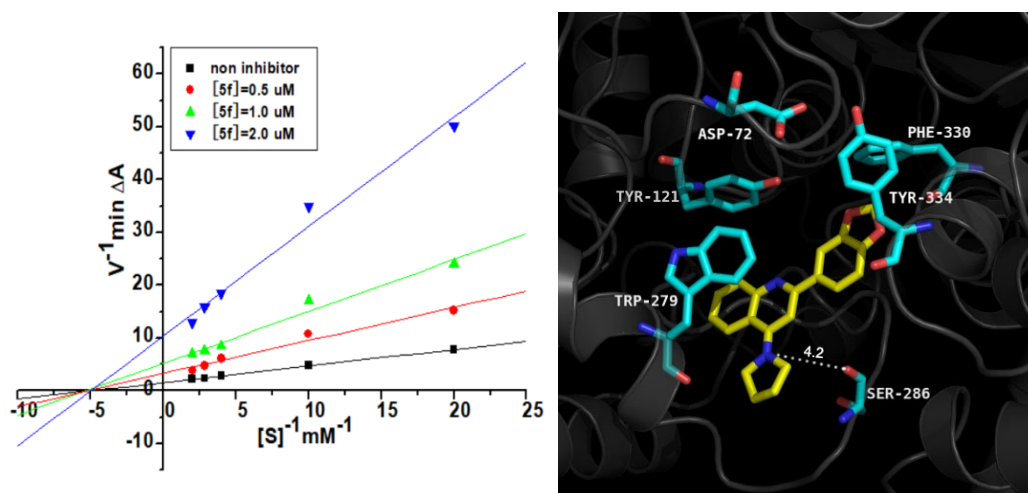


**Figure 2.** Lineweaver–Burk plot and docking model for compound **5f** with AChE.

## 2.4 Molecular modeling

To investigate the possible mode of compound **5f** with *TcAChE* (PDB code: 1ACJ), molecular modeling was carried out by AUTODOCK 4.0 package shown in Figure 2 [21]. In the **5f**-*TcAChE* complex, compound **5f** occupied the peripheral anionic site (PAS, Asp72, Trp279, Tyr121, Tyr334), the quinolone moiety establishes a cation- $\pi$  interaction with Trp279, the ring-to-ring distance was 4.0 Å, and the nitrogen atom of pyrrolidine had a hydrogen bond (4.2 Å) interaction with the carbonyl group of Ser286. The result showed that compound **5f** was able to bind PAS of AChE which was in agreement with the result of kinetic study.

## 2.5. Inhibition of self-mediated A $\beta_{1-42}$ aggregation by Thioflavin-T (ThT)

A $\beta_{1-42}$  and A $\beta_{1-40}$  are the main forms of A $\beta$  peptides found in amyloid plaques, A $\beta_{1-42}$  is more fibrillogenic than A $\beta_{1-40}$  [22], which inspired us to select A $\beta_{1-42}$  for evaluating the inhibitory activities of the derivatives using a ThT assay. The results suggested that these derivatives prevented self-

mediated A $\beta_{1-42}$  aggregation with percentages of inhibition ranging from 29-66% at 20  $\mu$ M. The most potent compounds were **5d-f** and **6d-f**, with percentages of inhibition greater than 50%, which were better than the reference compound curcumin (52%, Table 1). Compounds **5a-c**, **6a-c** and **5h** coupled with alkamines or n-butylamine showed moderate or low inhibitory activity. These results implied that side chain moiety gave a big influence resulting in the inhibitory activity for A $\beta_{1-42}$  aggregation.

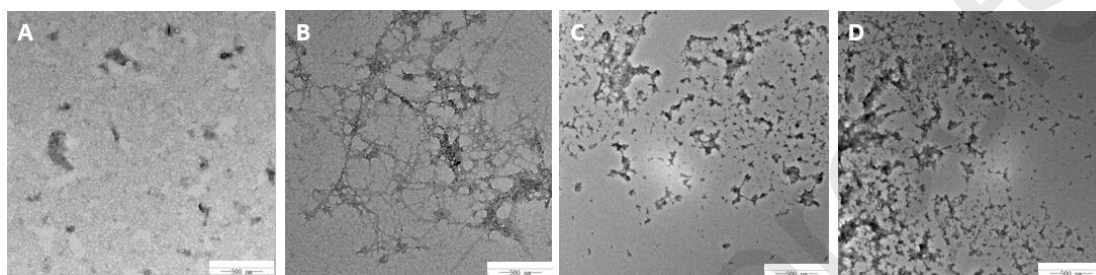


**Figure 3.** TEM images of A $\beta_{1-42}$  self-induced aggregation in the presence and absence of test compounds. (A) 50  $\mu$ M A $\beta_{1-42}$  without inhibitors at 0 h, (B) 50  $\mu$ M A $\beta_{1-42}$  without inhibitors at 48 h, 37 °C, (C) 50  $\mu$ M A $\beta_{1-42}$  and 20  $\mu$ M **5f**, (D) 50  $\mu$ M A $\beta_{1-42}$  and 20  $\mu$ M curcumin.

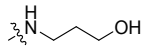
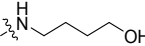
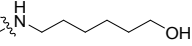
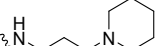
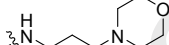
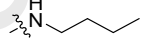
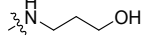
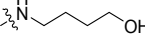
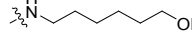
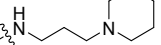
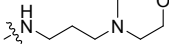
Compound **5f** showed considerably potent inhibition for both ChEs and A $\beta$  aggregation, therefore, it was selected as a representative compound and further evaluated by Transmission Electron Microscopic (TEM) study on A $\beta_{1-42}$  aggregation potential. Fig 3A represents the A $\beta_{1-42}$  aggregation at the start of the incubation at 37 °C without any inhibitor. After 48 h of incubation, the A $\beta_{1-42}$  had mostly aggregated into a firm and dense amyloid fibrils (Figure 3B). The inhibitory effect was clear when treated with the compound **5f** at 48 h (20  $\mu$ M) and lesser numbers of A $\beta$  aggregates were visible (Figure 3C) compared to the treatment with standard curcumin (Figure 3D). The results of TEM are consistent with the ThT assay where compound **5f** potentially inhibit A $\beta$  self-induced aggregation.

## 2.6. In vitro cytotoxicity

Tacrine, a well-known AChE inhibitor, was withdrawn from the market for its severe reversible hepatotoxicity. Our compounds' structure are similar to tacrine, therefore, to investigate the effect of

the target compounds on cell viability, MTT assay was performed using the human hepatoma cell line HepG2 and the rat pheochromocytoma cell line PC12. The results showed that most of the compounds (except for **5d**, **6d** and **6f**) exhibited no obvious toxicity with inhibition rate less than 20% on cell viability at 10  $\mu\text{M}$ . Among them, the  $\text{IC}_{50}$  of compounds **5a**, **5c**, **5f**, **5g**, **6a**, and **6b** were more than 50  $\mu\text{M}$  for both HepG2 and PC12 cell lines, it means they didn't show obvious toxicity at concentration of 50  $\mu\text{M}$  (Table 2).

**Table 2.** Inhibition rate (%)<sup>a</sup> and  $\text{IC}_{50}$ <sup>b</sup> of HepG2 and PC12 cells

Comps.	$\text{NR}_2\text{R}_3$	HepG2		PC12	
		10 $\mu\text{M}$ Inhibition (%)	$\text{IC}_{50}$ ( $\mu\text{M}$ )	10 $\mu\text{M}$ Inhibition (%)	$\text{IC}_{50}$ ( $\mu\text{M}$ )
<b>5a</b>		<5	>50	8.38 $\pm$ 0.12	>50
<b>5b</b>		<5	>50	14.68 $\pm$ 0.13	34.26 $\pm$ 2.48
<b>5c</b>		<5	>50	<5	>50
<b>5d</b>		43.70 $\pm$ 0.72	9.21 $\pm$ 1.98	71.47 $\pm$ 0.12	7.17 $\pm$ 2.35
<b>5e</b>		<5	17.71 $\pm$ 2.34	<5	>50
<b>5f</b>		<5	>50	<5	>50
<b>5g</b>		<5	>50	<5	>50
<b>5h</b>		15.44 $\pm$ 0.82	>50	11.24 $\pm$ 0.88	46.24 $\pm$ 3.08
<b>6a</b>		<5	>50	<5	>50
<b>6b</b>		<5	>50	<5	>50
<b>6c</b>		12.03 $\pm$ 0.34	44.19 $\pm$ 2.87	<5	>50
<b>6d</b>		24.1 $\pm$ 1.33	25.74 $\pm$ 2.45	11.55 $\pm$ 0.16	40.50 $\pm$ 2.49
<b>6e</b>		12.71 $\pm$ 0.93	30.06 $\pm$ 3.63	12.56 $\pm$ 0.19	35.23 $\pm$ 2.71

<b>6f</b>		12.6 ± 0.44	30.86 ± 1.66	24.22 ± 0.85	24.74 ± 1.83
Graveoline	-	8.76 ± 0.63	>50	<5	>50

<sup>a</sup>Inhibition rate =  $(A_{\text{Control}} - A_{\text{Sample}}) / (A_{\text{Control}} - A_{\text{Blank}}) \times 100\%$ , <sup>b</sup>IC<sub>50</sub> values represented the concentration causing 50% growth inhibition after treatment for 48 h. The values are the mean ± SD of three independent experiments.

## 2.7. ADMET prediction

The *in silico* prediction of the physicochemical and Absorption, Distribution, Metabolism, Elimination, and Toxicity (ADMET) properties of compound **5f** were calculated using the ACD/Labs Percepta Platform [23] (License#58830) and the results were compared to those obtained for donepezil and tacrine. As shown in Table 3, the compound **5f** had a similar druglikeness to donepezil, with no violations of Lipinski's rule of five. The solubility of compounds **5f** was calculated as 0.01 mg/mL, however, it was determined that the solubility of **5f** in PBS (0.1 mM, pH=7.4) was 0.26 mg/mL. In addition, compound **5f** was showed to be highly or moderately permeable based on the predicted Log P, permeability across Caco-2 monolayers (Pe) and human intestinal absorption (HIA) test. The score of compounds' Toxicity was predicted as undefined (score > 0.33 and < 0.67), so the data was not shown.

**Table 3.** Physico-chemistry properties and ADMET profile of compounds **5f**, donepezil and tacrine calculated using the Program ACD/Percepta.

Predicted properties	Compounds		
	<b>5f</b>	Donepezil	Tacrine
MW (g/mol)	317.38	379.49	198.26
H-Donors	0	0	2
H-Acceptor	3	4	2
Rot. Bonds	2	6	0
Rings	5	4	3
Lipinski	0	0	0
Solubility	0.01mg/mL	6.43 mg/mL	6 mg/mL
Log P	4.69	4.23	2.86

Caco-2	$P_e=237\times 10^{-6}$ cm/s	$P_e=194\times 10^{-6}$ cm/s	$P_e=63\times 10^{-6}$ cm/s
PPB	99%	95%	78%
CNS	-2.98	-2.65	-2.59
HIA	100%	100%	100%

## 2.8. Behavioral studies

Cognition-improving potency is utmost importance for anti-AD agents. The *in vitro* cholinesterase inhibitory activities must translate into behavioral effects and improve the cognition *in vivo*. The ameliorating potential of **5f** against scopolamine-induced cognition impairment in ICR mice was investigated in MWM [24]. The results show that the treatment with **5f** (20  $\mu$ mol/kg body weight) significantly ameliorated the cognition impairment in mice (Figure 4). In MWM test, mice in control group exhibited a reduction of mean escape latency from 62.2 to 42.3s ( $p < 0.01$ ) over the course of 4 training days. Compared to the model group, the **5f**-treated and THA-treated group showed significantly shortened escape latency in the 4th day of training trial sessions ( $p < 0.05$ ); the compound **5f** reduced the mean escape latency (MEL) from 60.2 to 48.1 s while THA decreased the MEL from 59.8 to 48.3 s ( $p < 0.05$ ) (Figure 4A). Furthermore, in the probe trial on day 15, the administration of **5f** significantly improved the overall target quadrant preference (the number to cross the platform, the percentage of path length in the target quadrant, and the swimming time in the target quadrant) compared to the model group ( $p < 0.05$ ) (Figure 4B–D), while no significant differences were observed between the two groups in the total distance traveled and swimming speed (Supporting Information, Figure S3). These results indicate that **5f** significantly ameliorated the cognition impairment in the scopolamine treated mice probably by penetrating the blood–brain barrier to affect the central nervous system.

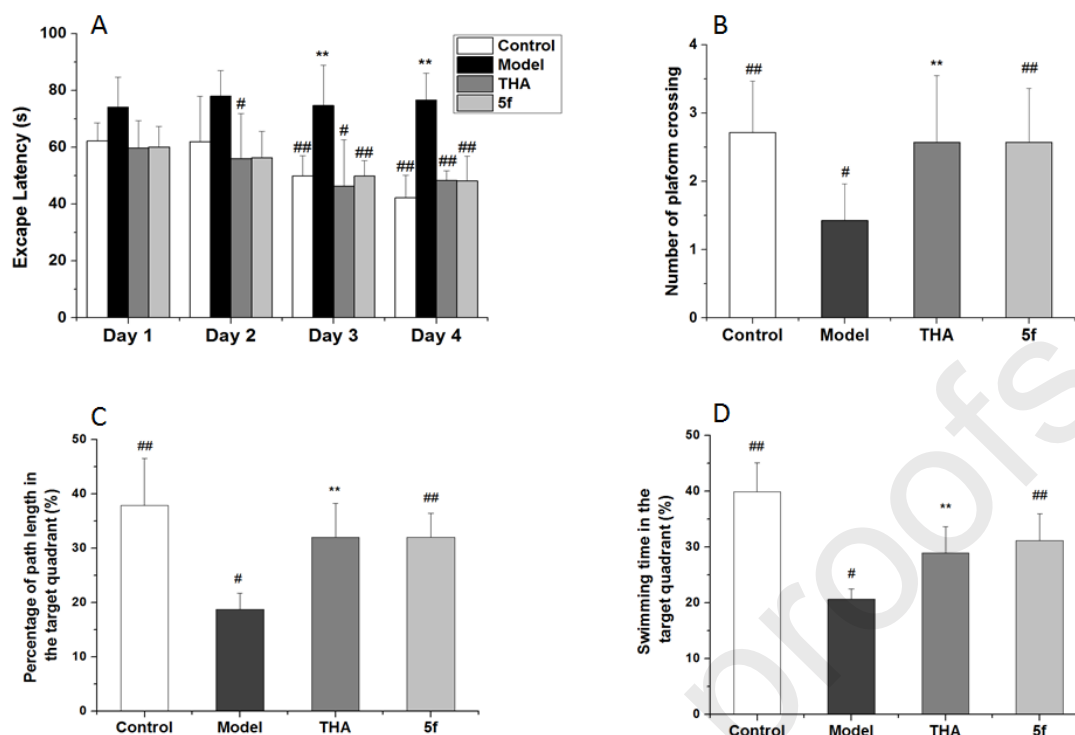


**Figure 4.** Effect of **5f** treatment on spatial memory performance. (A) Escape latencies during acquisition training trials measured for 90 s for each trial; (B) The number to cross the platform in probe trial without platform; (C) The percentage of path length in the target quadrant measured for 90 s in probe trial without platform; (D) The swimming time in the target quadrant measured for 90 s in probe trial without platform. Data are presented as mean  $\pm$  S.D. (n=8; \* $p$ <0.05, \*\* $p$ <0.01 vs control group, and # $p$ <0.05, ## $p$ <0.01 vs model group).

### 3. Conclusion

In conclusion, a series of graveoline derivatives were synthesized and evaluated for anti-AD agents. Among these compounds **5a-h** and **6c-e** were novel. The results demonstrated that most of these compounds exhibited moderate inhibitory activities against AChE and BuChE, with  $IC_{50}$  values in the sub-micromolar range. In particular, compound **5f** exhibited the best inhibitory activity for AChE and had surprisingly potent inhibitory activity for BuChE, which is remarkably stronger than Rivastigmine. Lineweaver-Burk plot and molecular modeling studies indicated compound **5f** showed a non-competitive inhibition with AChE. These derivatives also showed significant self-induced A $\beta$

aggregation inhibition. In addition, **5f** had a druglikeness similar to donepezil as calculated by ACD, with no violations of Lipinski's rule of five. The derivative **5f** didn't show obvious toxicity towards HepG2 and PC12 cell lines at 50  $\mu$ M. Furthermore, administration of **5f** considerably ameliorated the cognition impairment in the scopolamine treated ICR mice in MWM test.

Taking together, these graveolinine derivatives especially **5f** could be a promising lead compound for further development of newer anti-AD drugs.

## 4. Experimental section

### 4.1 Chemistry

All chemicals (reagent grade) were purchased from J&K and Sigma-Aldrich (China). Graveolinine was synthesized in our lab (Supporting Information). Flash column chromatography was performed with silica gel (200 - 300 mesh) purchased from Qingdao Haiyang Chemical Co. Ltd. Melting points (mp) were determined using an X-6 hot stage microscope and were not corrected.  $^1\text{H}$  and  $^{13}\text{C}$  NMR spectra data were obtained from a Bruker AV-300 or Bruker AV-400 spectrometer at 300 or 400 MHz and 75 or 100 MHz, respectively. MS spectra were recorded on a Shimadzu LCMS-2010A instrument with an ESI mass selective detector. Elemental analyses were performed on a Gmbe VarioEL Elemental Instrument.

### 4.2 General procedure for the synthesis of the intermediates (2a, 2b)

To a mixture of **1** (1.35 g, 10.0 mmol) and  $\text{Et}_3\text{N}$  (10 mL) in  $\text{CH}_2\text{Cl}_2$  (100 mL) was added slowly piperonyl chloride or benzoyl chloride (11.0 mmol) at room temperature. The mixture was stirred for 24 h and poured into 100 mL ice water. The precipitate was collected and washed with water and then with methanol, the solid was dried under vacuum and used without further purification.

### 4.3 General procedure for the synthesis of the intermediates (3a, 3b)

The solid above (**2a** or **2b**) was suspended in 150 mL of *tert*-butyl alcohol. Potassium *tert*-butoxide (15.0 g, 134 mmol) was added, and the mixture was heated at 75 °C for 16 h. The mixture was cooled and poured into 50 mL of ice water. 10% aqueous HCl was added until pH=6. The solid was collected and washed with water three times. The crude product was recrystallized from CH<sub>2</sub>Cl<sub>2</sub> and petroleum and afforded the **3a** or **3b**. Intermediates (**3a** and **3b**) were routinely checked by TLC and <sup>1</sup>H NMR, and subjected to the subsequent synthesis without further purification.

#### 2-(benzo[d][1,3]dioxol-5-yl)quinolin-4(1H)-one (**3a**)

Dark yellow crystal, yield: 80%. <sup>1</sup>H NMR (400 MHz, DMSO-*d*<sub>6</sub>) δ 8.24 (d, *J* = 8.4 Hz, 2H, 2×Ar-H), 7.95 (t, *J* = 7.8 Hz, 1H, Ar-H), 7.65 (t, *J* = 7.2 Hz, 1H, Ar-H), 7.60 (d, *J* = 1.8 Hz, 1H, Ar-H), 7.52 (d, *J* = 8.0 Hz, 1H, ×Ar-H), 7.31 – 7.13 (m, 2H, 2×Ar-H), 6.20 (s, 2H, OCH<sub>2</sub>O), 5.51 (s, 1H, NH).

#### 2-phenylquinolin-4(1H)-one (**3b**)

Light yellow crystal, yield: 82%, <sup>1</sup>H NMR (400 MHz, DMSO-*d*<sub>6</sub>) δ 8.10 (d, *J* = 8.0 Hz, 1H, Ar-H), 7.86 (d, *J* = 3.6 Hz, 1H, Ar-H), 7.84 (d, *J* = 2.2 Hz, 1H, Ar-H), 7.81 (d, *J* = 8.4 Hz, 1H, Ar-H), 7.67 (t, *J* = 7.6 Hz, 1H, Ar-H), 7.59 (s, 1H, Ar-H), 7.58 (d, *J* = 2.6 Hz, 2H, 2×Ar-H), 7.34 (t, *J* = 7.6 Hz, 1H, Ar-H), 6.36 (s, 1H, Ar-H).

#### 4.4 General procedure for the synthesis of the intermediates (**4a**, **4b**)

Compound **3** (10 mmol) and POCl<sub>3</sub> (50 mL) were stirred in ice bath for 30 min, and refluxed for further 4 h. After cooling, the mixture was poured into 200 mL of ice water. The saturated solution of NaOH was added until pH=7. The mixture was extracted with CH<sub>2</sub>Cl<sub>2</sub> (3 × 100 mL), and the combined organic layer was dried with MgSO<sub>4</sub> and evaporated. The crude residue was purified by silica gel column chromatography using CH<sub>2</sub>Cl<sub>2</sub>-petroleum (1:5) as an eluent to afford **4a** or **4b**.

#### 2-(benzo[d][1,3]dioxol-5-yl)-4-chloroquinoline (**4a**)

Light white feathery crystal, Yield: 41%, m.p. 63-65 °C. <sup>1</sup>H NMR (300 MHz, Chloroform-*d*)  $\delta$  8.17 (t,  $J = 7.5$  Hz, 2H, 2 $\times$ Ar-H), 7.86 (s, 1H, Ar-H), 7.75 (t,  $J = 7.8$  Hz, 1H, Ar-H), 7.70 (s, 1H, Ar-H), 7.65 – 7.57 (m, 2H, Ar-H), 6.93 (d,  $J = 8.1$  Hz, 1H, Ar-H), 6.04 (s, 2H, OCH<sub>2</sub>O).

#### 4-chloro-2-phenylquinoline (**4b**)

Pale solid, Yield: 56%, m.p. 122-124 °C. <sup>1</sup>H NMR (300 MHz, Chloroform-*d*)  $\delta$  8.36 (d,  $J = 8.4$  Hz, 1H, Ar-H), 8.25 (d,  $J = 8.4$  Hz, 1H, Ar-H), 8.17 (d,  $J = 7.2$  Hz, 2H, 2 $\times$ Ar-H), 7.99 (s, 1H, Ar-H), 7.82 (t,  $J = 7.5$  Hz, 1H, Ar-H), 7.70 – 7.62 (m, 1H, Ar-H), 7.58 - 7.48 (m, 3H, 3 $\times$ Ar-H).

### 4.5 General procedure for the synthesis of the target compounds (**5a-5h**, **6a-6f**)

A mixture of intermediates (**4a** or **4b**, 1 mmol), K<sub>2</sub>CO<sub>3</sub> (2 mmol) and amine (2 mmol) were stirred at 135 °C under for 4 h. After cooling, 10 mL of distilled water was added, the precipitate was filtered and dried, then purified by silica gel column chromatography using CH<sub>2</sub>Cl<sub>2</sub>/MeOH (20:1) as an eluent.

#### 4.5.1 3-((2-(benzo[d][1,3]dioxol-5-yl)quinolin-4-yl)amino)propan-1-ol (**5a**)

Sandybrown solid, yield: 51%, m.p. 126-128 °C. <sup>1</sup>H NMR (300 MHz, Methanol-*d*<sub>4</sub>)  $\delta$  8.00 (d,  $J = 8.4$  Hz, 1H, Ar-H), 7.87 (d,  $J = 8.4$  Hz, 1H, Ar-H), 7.61 (t,  $J = 7.8$  Hz, 1H, Ar-H), 7.46 – 7.35 (m, 3H, 3 $\times$ Ar-H), 6.90 (d,  $J = 8.7$  Hz, 1H, Ar-H), 6.75 (s, 1H, Ar-H), 5.99 (s, 2H, OCH<sub>2</sub>O), 3.75 (t,  $J = 6.0$  Hz, 2H, CH<sub>2</sub>), 3.49 (t,  $J = 7.0$  Hz, 2H, CH<sub>2</sub>), 1.98 (p,  $J = 6.4$  Hz, 2H, CH<sub>2</sub>). <sup>13</sup>C NMR (75 MHz, Methanol-*d*<sub>4</sub>)  $\delta$  157.9, 151.8, 148.7, 148.1, 147.1, 134.3, 129.5, 127.0, 124.0, 121.7, 120.5, 117.8, 107.8, 107.7, 101.4, 95.8, 59.5, 40.0, 30.9. ESI-MS  $m/z$ : 323.2 [M+H]<sup>+</sup>. Elemental Anal. Calcd for C<sub>19</sub>H<sub>18</sub>N<sub>2</sub>O<sub>3</sub>: C, 70.79; H, 5.63; N, 8.69. Found: C, 71.06; H, 5.83; N, 8.41.

#### 4.5.2 4-((2-(benzo[d][1,3]dioxol-5-yl)quinolin-4-yl)amino)butan-1-ol (**5b**)

Sandybrown solid, yield: 62.2%, m.p. 118-120 °C. <sup>1</sup>H NMR (300 MHz, Methanol-*d*<sub>4</sub>)  $\delta$  8.07 (d,  $J = 8.4$  Hz, 1H, Ar-H), 7.89 (d,  $J = 8.1$  Hz, 1H, Ar-H), 7.62 (t,  $J = 7.8$  Hz, 1H, Ar-H), 7.48 – 7.44 (m,

2H, 2×Ar-H), 7.40 (t,  $J = 7.5$  Hz, 1H, Ar-H), 6.93 (d,  $J = 8.7$  Hz, 1H, Ar-H), 6.74 (s, 1H, Ar-H), 6.02 (s, 2H, OCH<sub>2</sub>O), 3.65 (t,  $J = 6.3$  Hz, 2H, CH<sub>2</sub>), 3.43 (t,  $J = 6.9$  Hz, 2H, CH<sub>2</sub>), 1.91 – 1.81 (m, 2H, CH<sub>2</sub>), 1.76 – 1.67 (m, 2H, CH<sub>2</sub>). <sup>13</sup>C NMR (75 MHz, Methanol-*d*<sub>4</sub>)  $\delta$  158.3, 151.6, 148.7, 148.1, 147.6, 134.8, 129.3, 127.4, 123.9, 121.6, 120.6, 117.9, 107.8, 107.7, 101.4, 95.9, 61.2, 42.5, 29.8, 24.7. ESI-MS  $m/z$ : 337.2 [M+H]<sup>+</sup>. Elemental Anal. Calcd for C<sub>20</sub>H<sub>20</sub>N<sub>2</sub>O<sub>3</sub>: C, 71.41; H, 5.99; N, 8.33. Found: C, 71.61; H, 5.65; N, 8.18.

#### 4.5.3 6-((2-(benzo[d][1,3]dioxol-5-yl)quinolin-4-yl)amino)hexan-1-ol (**5c**)

Sandybrown oil, yield: 59.8%. <sup>1</sup>H NMR (300 MHz, Acetone-*d*<sub>6</sub>)  $\delta$  8.13 (d,  $J = 8.1$  Hz, 1H, Ar-H), 7.90 (d,  $J = 8.4$  Hz, 1H, Ar-H), 7.84 – 7.76 (m, 2H, 2×Ar-H), 7.60 (t,  $J = 7.5$  Hz, 1H, Ar-H), 7.36 (t,  $J = 7.5$  Hz, 1H, Ar-H), 7.01 (s, 1H, Ar-H), 6.95 (d,  $J = 8.1$  Hz, 1H, Ar-H), 6.49 (t,  $J = 4.5$  Hz, 1H, NH), 6.07 (s, 2H, OCH<sub>2</sub>O), 3.55 – 3.48 (m, 4H, 2×CH<sub>2</sub>), 2.97 (brs, 1H), 1.86 – 1.78 (m, 2H, CH<sub>2</sub>), 1.55 – 1.46 (m, 6H, 3×CH<sub>2</sub>). <sup>13</sup>C NMR (75 MHz, Acetone-*d*<sub>6</sub>)  $\delta$  156.5, 150.9, 148.7, 148.4, 148.1, 135.2, 129.7, 128.8, 123.6, 121.2, 120.6, 118.3, 107.9, 107.5, 101.4, 94.9, 61.5, 42.9, 32.85, 28.5, 27.0, 25.7. ESI-MS  $m/z$ : 365.2 [M+H]<sup>+</sup>. Elemental Anal. Calcd for C<sub>22</sub>H<sub>24</sub>N<sub>2</sub>O<sub>3</sub>: C, 72.51; H, 6.64; N, 7.69. Found: C, 72.23; H, 6.67; N, 7.35.

#### 4.5.4 2-(benzo[d][1,3]dioxol-5-yl)-N-(3-(piperidin-1-yl)propyl)quinolin-4-amine (**5d**)

Sandybrown solid, yield: 79%, m.p. 109-111 °C. <sup>1</sup>H NMR (300 MHz, Methanol-*d*<sub>4</sub>)  $\delta$  8.16 (d,  $J = 8.1$  Hz, 1H, Ar-H), 7.91 (d,  $J = 8.1$  Hz, 1H, Ar-H), 7.71 (t,  $J = 7.8$  Hz, 1H, Ar-H), 7.53 – 7.45 (m, 3H, 3×Ar-H), 6.98 (d,  $J = 7.9$  Hz, 1H, Ar-H), 6.81 (s, 1H, Ar-H), 6.06 (s, 2H, OCH<sub>2</sub>O), 3.56 (t,  $J = 6.9$  Hz, 2H, CH<sub>2</sub>), 2.80 – 2.72 (m, 6H, 3×CH<sub>2</sub>), 2.12 – 2.03 (m, 2H, CH<sub>2</sub>), 1.75 – 1.68 (m, 4H, 2×CH<sub>2</sub>), 1.60 – 1.54 (m, 2H, CH<sub>2</sub>). <sup>13</sup>C NMR (75 MHz, Methanol-*d*<sub>4</sub>)  $\delta$  157.1, 152.4, 149.2, 148.2, 145.6, 132.8, 130.3, 125.8, 124.5, 122.0, 121.0, 117.5, 108.0, 107.7, 101.6, 96.0, 56.3, 53.9, 41.1, 24.7, 24.1, 23.2. ESI-MS

$m/z$ : 390.2  $[M+H]^+$ . Elemental Anal. Calcd for  $C_{24}H_{27}N_3O_2$ : C, 74.01; H, 6.99; N, 10.79. Found: C, 73.93; H, 6.79; N, 11.07.

#### 4.5.5 2-(benzo[d][1,3]dioxol-5-yl)-N-(3-morpholinopropyl)quinolin-4-amine (**5e**)

Sandybrown solid, yield: 82.8%, m.p. 142-144 °C.  $^1H$  NMR (300 MHz, Chloroform- $d$ )  $\delta$  8.19 (d,  $J = 8.1$  Hz, 1H, Ar-H), 7.97 (d,  $J = 8.1$  Hz, 1H, Ar-H), 7.60 (d,  $J = 8.1$  Hz, 2H, 2 $\times$ Ar-H), 7.55 (s, 1H, Ar-H), 7.40 (t,  $J = 6.9$  Hz, 1H, Ar-H), 6.86 (d,  $J = 7.8$  Hz, 1H, Ar-H), 6.64 (s, 1H, Ar-H), 5.98 (s, 2H, OCH<sub>2</sub>O), 3.83 (s, 4H, CH<sub>2</sub>), 3.52 (s, 2H, CH<sub>2</sub>), 2.71 – 2.47 (m, 6H, 3 $\times$ CH<sub>2</sub>), 1.99 (s, 2H, CH<sub>2</sub>).  $^{13}C$  NMR (75 MHz, Chloroform- $d$ )  $\delta$  156.5, 152.0, 149.0, 148.1, 145.9, 132.8, 130.1, 127.7, 124.5, 122.3, 120.6, 117.6, 108.4, 108.2, 101.5, 95.9, 66.9, 58.7, 54.0, 44.1, 30.0, 29.7, 23.5. ESI-MS  $m/z$ : 392.2  $[M+H]^+$ . Elemental Anal. Calcd for  $C_{23}H_{25}N_3O_3$ : C, 70.57; H, 6.44; N, 10.73. Found: C, 70.65; H, 6.35; N, 10.81.

#### 4.5.6 2-(benzo[d][1,3]dioxol-5-yl)-4-(pyrrolidin-1-yl)quinoline (**5f**)

Sandybrown solid, yield: 88.0%, m.p. 165-167 °C.  $^1H$  NMR (300 MHz, Chloroform- $d$ )  $\delta$  8.15 (d,  $J = 8.7$  Hz, 1H, Ar-H), 8.08 (d,  $J = 8.4$  Hz, 1H, Ar-H), 7.61 – 7.54 (m, 3H, 3 $\times$ Ar-H), 7.31 – 7.25 (m, 1H, Ar-H), 6.90 (d,  $J = 8.1$  Hz, 1H, Ar-H), 6.76 (s, 1H, Ar-H), 5.99 (s, 2H, OCH<sub>2</sub>O), 3.73 – 3.64 (m, 4H, 2 $\times$ CH<sub>2</sub>), 2.07 – 1.97 (m, 4H, 2 $\times$ CH<sub>2</sub>).  $^{13}C$  NMR (75 MHz, Chloroform- $d$ )  $\delta$  152.2, 149.6, 144.6, 144.1, 125.2, 125.0, 121.0, 119.1, 117.9, 116.0, 104.4, 104.2, 97.4, 96.3, 48.4, 22.0. ESI-MS  $m/z$ : 319.1  $[M+H]^+$ . Elemental Anal. Calcd for  $C_{20}H_{18}N_2O_2$ : C, 75.45; H, 5.70; N, 8.80. Found: C, 75.62; H, 5.36; N, 8.80.

#### 4.5.7 2-(benzo[d][1,3]dioxol-5-yl)-4-(piperidin-1-yl)quinoline (**5g**)

Sandybrown solid, yield: 62.6%, m.p. 143-146 °C.  $^1H$  NMR (300 MHz, Chloroform- $d$ )  $\delta$  8.10 (d,  $J = 8.4$  Hz, 1H, Ar-H), 7.99 (d,  $J = 8.4$  Hz, 1H, Ar-H), 7.70 (s, 1H, Ar-H), 7.63 (t,  $J = 8.4$  Hz, 2H, 2 $\times$ Ar-

H), 7.42 (t,  $J = 7.5$  Hz, 1H, Ar-H), 7.19 (s, 1H, Ar-H), 6.93 (d,  $J = 8.1$  Hz, 1H, Ar-H), 6.01 (s, 2H, OCH<sub>2</sub>O), 3.25 – 3.14 (m, 4H, 2×CH<sub>2</sub>), 1.85 (p,  $J = 6.0$  Hz, 4H, 2×CH<sub>2</sub>), 1.73 – 1.64 (m, 2H, CH<sub>2</sub>). <sup>13</sup>C NMR (75 MHz, Chloroform-*d*)  $\delta$  158.6, 157.4, 149.5, 148.6, 148.2, 134.9, 130.0, 129.1, 124.7, 123.7, 122.7, 121.7, 108.4, 108.0, 106.3, 101.3, 53.7, 26.2, 24.5. ESI-MS  $m/z$ : 333.2 [M+H]<sup>+</sup>. Elemental Anal. Calcd for C<sub>21</sub>H<sub>20</sub>N<sub>2</sub>O<sub>2</sub>: C, 75.88; H, 6.06; N, 8.43. Found: C, 75.71; H, 5.91; N, 8.32.

#### 4.5.8 2-(benzo[*d*][1,3]dioxol-5-yl)-*N*-butylquinolin-4-amine (**5h**)

Sandybrown solid, yield: 55.24%, m.p. 86-88 °C. <sup>1</sup>H NMR (300 MHz, Chloroform-*d*)  $\delta$  8.04 (d,  $J = 8.4$  Hz, 1H, Ar-H), 7.70 (d,  $J = 8.1$  Hz, 1H, Ar-H), 7.64 (s, 1H, Ar-H), 7.60 (d,  $J = 8.1$  Hz, 2H, 2×Ar-H), 7.37 (t,  $J = 7.5$  Hz, 1H, Ar-H), 6.92 (d,  $J = 8.1$  Hz, 1H, Ar-H), 6.76 (s, 1H, Ar-H), 6.01 (s, 2H, OCH<sub>2</sub>O), 3.39 – 3.32 (m, 2H, CH<sub>2</sub>), 1.76 (p,  $J = 7.2$  Hz, 2H, CH<sub>2</sub>), 1.58 – 1.45 (m, 2H, CH<sub>2</sub>), 1.01 (t,  $J = 7.2$  Hz, 3H, CH<sub>3</sub>). <sup>13</sup>C NMR (75 MHz, Chloroform-*d*)  $\delta$  157.7, 150.2, 148.4, 148.4, 148.1, 135.3, 130.0, 129.2, 124.2, 121.6, 119.1, 117.7, 108.3, 108.1, 101.3, 96.2, 43.0, 31.1, 20.4, 13.9. ESI-MS  $m/z$ : 321.2 [M+H]<sup>+</sup>. Elemental Anal. Calcd for C<sub>20</sub>H<sub>20</sub>N<sub>2</sub>O<sub>2</sub>: C, 74.98; H, 6.29; N, 8.74. Found: C, 74.63; H, 6.55; N, 8.41.

#### 4.5.9 3-((2-phenylquinolin-4-yl)amino)propan-1-ol (**6a**)

Sandybrown solid, Yield: 51%, m.p. 134-137 °C. <sup>1</sup>H NMR (300 MHz, Acetone-*d*<sub>6</sub>)  $\delta$  8.28 (d,  $J = 6.9$  Hz, 2H, 2×Ar-H), 8.11 (d,  $J = 7.8$  Hz, 1H, Ar-H), 8.00 (d,  $J = 8.4$  Hz, 1H, Ar-H), 7.66 (t,  $J = 7.5$  Hz, 1H, Ar-H), 7.52 (t,  $J = 7.2$  Hz, 2H, 2×Ar-H), 7.49 – 7.39 (m, 2H, 2×Ar-H), 7.12 (s, 1H, Ar-H), 6.81 (s, 1H, NH), 3.83 (t,  $J = 5.7$  Hz, 2H, CH<sub>2</sub>), 3.67 – 3.61 (m, 2H, CH<sub>2</sub>), 3.51 (brs, 1H, OH), 2.09 – 2.05 (m, 2H). <sup>13</sup>C NMR (75 MHz, Acetone-*d*<sub>6</sub>)  $\delta$  157.3, 151.1, 148.7, 140.8, 129.7, 129.0, 128.8, 128.3, 127.3, 124.0, 120.6, 118.4, 95.4, 60.0, 40.7, 31.3. ESI-MS  $m/z$ : 279.1 [M+H]<sup>+</sup>. Elemental Anal. Calcd for C<sub>18</sub>H<sub>18</sub>N<sub>2</sub>O: C, 77.67; H, 6.52; N, 10.06. Found: C, 77.55; H, 6.70; N, 10.35.

4.5.10 4-((2-phenylquinolin-4-yl)amino)butan-1-ol (**6b**)

Sandybrown solid, yield:75.0%, m.p. 132-134 °C. <sup>1</sup>H NMR (300 MHz, Acetone-*d*<sub>6</sub>) δ 8.26 (d, *J* = 6.9 Hz, 2H, 2×Ar-H), 8.15 (d, *J* = 8.4 Hz, 1H, Ar-H), 7.96 (d, *J* = 8.4 Hz, 1H, Ar-H), 7.62 (t, *J* = 7.5 Hz, 1H, Ar-H), 7.49 (t, *J* = 7.2 Hz, 2H, 2×Ar-H), 7.43 (d, *J* = 6.9 Hz, 1H, Ar-H), 7.38 (t, *J* = 7.5 Hz, 1H, Ar-H), 7.07 (s, 1H, Ar-H), 6.66 (s, 1H, NH), 3.65 (t, *J* = 6.3 Hz, 2H, CH<sub>2</sub>), 3.55 – 3.48 (m, 2H, CH<sub>2</sub>), 1.91 (p, *J* = 6.9 Hz, 2H, CH<sub>2</sub>), 1.77 – 1.66 (m, 2H, CH<sub>2</sub>). <sup>13</sup>C NMR (75 MHz, Acetone-*d*<sub>6</sub>) δ 157.2, 151.1, 148.8, 140.8, 129.8, 128.9, 128.7, 128.3, 127.3, 123.9, 120.7, 118.4, 95.4, 61.3, 42.9, 30.3, 25.1. ESI-MS *m/z*: 293.1 [M+H]<sup>+</sup>. Elemental Anal. Calcd for C<sub>19</sub>H<sub>20</sub>N<sub>2</sub>O: C, 78.05; H, 6.90; N, 9.58. Found: C, 78.00; H, 6.57; N, 9.49.

4.5.11 6-((2-phenylquinolin-4-yl)amino)hexan-1-ol (**6c**)

Sandybrown solid, yield: 63.2%, m.p. 116-118 °C. <sup>1</sup>H NMR (300 MHz, Acetone-*d*<sub>6</sub>) δ 8.25 (d, *J* = 6.9 Hz, 2H, 2×Ar-H), 8.16 (d, *J* = 8.4 Hz, 1H, Ar-H), 7.97 (d, *J* = 8.4 Hz, 1H, Ar-H), 7.65 – 7.58 (m, 1H, Ar-H), 7.49 (t, *J* = 7.2 Hz, 2H, 2×Ar-H), 7.45 – 7.34 (m, 2H, 2×Ar-H), 7.06 (s, 1H, Ar-H), 6.56 (s, 1H, NH), 3.54 (t, *J* = 6.3 Hz, 2H, CH<sub>2</sub>), 3.49 – 3.44 (m, 2H, CH<sub>2</sub>), 1.85 – 1.76 (m, 2H, CH<sub>2</sub>), 1.58 – 1.39 (m, 6H, 3×CH<sub>2</sub>). <sup>13</sup>C NMR (75 MHz, Acetone-*d*<sub>6</sub>) δ 157.3, 151.1, 148.8, 140.8, 129.7, 128.9, 128.7, 128.3, 127.3, 123.9, 120.7, 118.4, 95.4, 61.5, 43.0, 32.9, 27.0, 25.7. ESI-MS *m/z*: 321.2 [M+H]<sup>+</sup>. Elemental Anal. Calcd for C<sub>21</sub>H<sub>24</sub>N<sub>2</sub>O: C, 78.71; H, 7.55; N, 8.74. Found: C, 78.82; H, 7.68; N, 8.98.

4.5.12 2-phenyl-N-(3-(piperidin-1-yl)propyl)quinolin-4-amine (**6d**)

Sandybrown solid, yield: 80.2%, m.p. 147-149 °C. <sup>1</sup>H NMR (300 MHz, Chloroform-*d*) δ 8.11 – 8.06 (m, 3H, 3×Ar-H), 7.95 (d, *J* = 8.4 Hz, 1H, Ar-H), 7.69 – 7.61 (m, 2H, 2×Ar-H), 7.50 (t, *J* = 7.2 Hz, 2H, 2×Ar-H), 7.44 (d, *J* = 7.2 Hz, 1H, Ar-H), 7.38 (d, *J* = 7.2 Hz, 1H, Ar-H), 6.77 (s, 1H, NH), 3.46 – 3.39 (m, 2H, CH<sub>2</sub>), 2.57 – 2.53 (m, 2H, CH<sub>2</sub>), 1.98 – 1.90 (m, 2H, CH<sub>2</sub>), 1.73 (q, *J* = 5.4 Hz,

4H, 2×CH<sub>2</sub>), 1.60 – 1.54 (m, 2H, CH<sub>2</sub>). <sup>13</sup>C NMR (75 MHz, Chloroform-*d*) δ 158.6, 151.2, 148.5, 141.2, 129.9, 129.0, 128.7, 128.5, 127.6, 127.5, 123.7, 120.7, 118.3, 96.0, 59.4, 55.0, 44.5, 26.0, 24.4, 23.6. ESI-MS *m/z*: 346.3 [M+H]<sup>+</sup>. Elemental Anal. Calcd for C<sub>23</sub>H<sub>27</sub>N<sub>3</sub>: C, 79.96; H, 7.88; N, 12.16. Found: C, 79.98; H, 7.83; N, 12.28.

#### 4.5.13 N-(3-morpholinopropyl)-2-phenylquinolin-4-amine (6e)

Sandybrown solid, yield: 79.5%, m.p. 152-154 °C. <sup>1</sup>H NMR (300 MHz, Chloroform-*d*) δ 7.97 (d, *J* = 7.8 Hz, 3H, 3×Ar-H), 7.75 (d, *J* = 8.4 Hz, 1H, Ar-H), 7.52 (t, *J* = 7.5 Hz, 1H, Ar-H), 7.37 (t, *J* = 7.2 Hz, 2H, 2×Ar-H), 7.29 (q, *J* = 7.5, 7.2 Hz, 2H, 2×Ar-H), 6.90 (t, *J* = 4.5 Hz, 1H, Ar-H), 6.65 (s, 1H, NH), 3.70 (t, *J* = 4.5 Hz, 4H, 2×CH<sub>2</sub>), 3.27 (q, *J* = 5.4 Hz, 2H, CH<sub>2</sub>), 2.45 - 2.37 (m, 6H, 3×CH<sub>2</sub>), 1.77 (p, *J* = 6.0 Hz, 2H, CH<sub>2</sub>). <sup>13</sup>C NMR (75 MHz, Chloroform-*d*) δ 158.5, 151.0, 148.6, 141.1, 130.1, 129.2, 128.8, 128.6, 127.6, 124.0, 120.2, 118.2, 96.2, 67.0, 58.8, 54.0, 44.0, 23.6. ESI-MS *m/z*: 348.2 [M+H]<sup>+</sup>. Elemental Anal. Calcd for C<sub>22</sub>H<sub>25</sub>N<sub>3</sub>O: C, 76.05; H, 7.25; N, 12.09. Found: C, 76.39; H, 7.47; N, 12.16.

#### 4.5.14 2-phenyl-4-(pyrrolidin-1-yl)quinoline (6f)

Sandybrown solid, yield: 78.9%, m.p. 166-169 °C. <sup>1</sup>H NMR (300 MHz, Chloroform-*d*) δ 8.45 (d, *J* = 8.1 Hz, 1H, Ar-H), 8.21 (d, *J* = 8.4 Hz, 1H, Ar-H), 8.09 (d, *J* = 1.8 Hz, 1H, Ar-H), 8.06 (d, *J* = 1.5 Hz, 1H, Ar-H), 7.62 (t, *J* = 7.8 Hz, 1H, Ar-H), 7.51 – 7.41 (m, 3H, 3×Ar-H), 7.34 (t, *J* = 7.8 Hz, 1H, Ar-H), 6.78 (s, 1H, Ar-H), 3.86 – 3.76 (m, 4H, 2×CH<sub>2</sub>), 2.13 – 2.05 (m, 4H, 2×CH<sub>2</sub>). <sup>13</sup>C NMR (75 MHz, Chloroform-*d*) δ 155.7, 153.9, 147.4, 138.1, 129.8, 129.6, 128.7, 127.9, 127.7, 125.0, 123.6, 119.4, 100.6, 52.6, 25.9. ESI-MS *m/z*: 275.1 [M+H]<sup>+</sup>. Elemental Anal. Calcd for C<sub>19</sub>H<sub>18</sub>N<sub>2</sub>: C, 83.18; H, 6.61; N, 10.21. Found: C, 83.43; H, 6.34; N, 10.02.

## 5. Biological activity

### 5.1. In vitro inhibition studies on AChE and BChE

AChE (E.C.3.1.1.7, Type VI-S, from *electric eel*) and BuChE (E.C.3.1.1.8, from equine serum), 5,5'-dithiobis-(2-nitrobenzoic acid) (DTNB), acetylthiocholine chloride (ATC), butylthiocholine chloride (BTC) were purchased from Sigma-Aldrich. The compounds were dissolved in a minimum volume of DMSO (1%) and diluted in phosphate-buffered solution (0.1 M, pH 8.0) to provide a final concentration range. All the assays were under the phosphate-buffered solution, using a Shimadzu UV-2450 Spectrophotometer. Enzyme solutions were prepared to give 2.0 units/mL in 2 mL aliquots. The assay medium contained 10  $\mu$ L of enzyme, 50  $\mu$ L of DTNB (0.01 M) and 50  $\mu$ L of substrate (ATC, 0.01 M). The substrate was added to the assay medium containing enzyme, buffer, and DTNB with inhibitor after 15 min of incubation time at 37 °C. The activity was determined by measuring the increase in absorbance at 412 nm at 1 min intervals at 37 °C. Calculations were performed according to the method of the equation in Ellman et al [19]. *In vitro* BuChE assay use the similar method described above. Each concentration was assayed in triplicate.

### 5.2. Kinetic characterization of AChE inhibition

Three different concentrations of substrate were mixed in the 1.0 mL phosphate buffer (0.1 M, pH 8.0), containing 50  $\mu$ L of DTNB, 10  $\mu$ L AChE, and 50  $\mu$ L substrate. Test compound was added into the assay solution and pre-incubated with the enzyme at 37°C for 15 min, followed by the addition of substrate. Kinetic characterization of the hydrolysis of ATC catalyzed by AChE was done spectrometrically at 412 nm. A parallel control with no inhibitor in the mixture, allowed adjusting activities to be measured at various times.

### 5.3. Molecular modeling

The crystal structure of the torpedo AChE (code ID: 1ACJ) were obtained in the Protein Data Bank after eliminating the inhibitor and water molecules. The 3D structure of **5f** was built and performed geometry optimization by molecular mechanics. Further preparation of substrates included addition of Gasteiger charges, removal of hydrogen atoms and addition of their atomic charges to skeleton atoms, and finally, assignment of proper atomic types. Autotors was then used to define the rotatable bonds in the ligand.

Docking studies were carried out using the AutoDock 4.2 program (The Scripps Research Institute, San Diego, CA, USA), polar hydrogen atoms were added and Gasteiger charges were assigned to the enzyme. The resulting enzyme structure was used as an input for the AUTOGRID program. AUTOGRID performed a precalculated atomic affinity grid maps for each atom type in the ligand plus an electrostatics map and a separate desolvation map present in the substrate molecule. All maps were calculated with 0.375 Å spacing between grid points. The center of the grid box was placed at the bottom of the active site gorge (AChE [2.781 64.383 67.971]). The dimensions of the active site box were set at 50 × 46 × 46 Å. Flexible ligand docking was performed for the compounds. Docking calculations were carried out using the Lamarckian genetic algorithm (LGA) and all parameters were the same for each docking. To ensure the reliability of the results, the docking procedures were repeated 10 independent times for the compounds and the obtained orientations were analyzed.

#### **5.4. Inhibition of self-mediated A $\beta$ (1-42) aggregation [25]**

A $\beta$ <sub>1-42</sub> peptide (Chinapeptides) was dissolved in ammonium hydroxide (1% v/v), and diluted with phosphate buffer (pH 7.40, 20 mM) to 200  $\mu$ M before use. Compounds were firstly dissolved in DMSO to obtain a 10 mM solution. The peptide was incubated in phosphate buffer (pH 7.40, 20 mM) in 37 °C for 48 h (final A $\beta$  concentration of 50  $\mu$ M) with or without the tested compounds at 20  $\mu$ M. After

incubation, thioflavin-T (5  $\mu$ M in 50 mM glycine-NaOH buffer, pH 8.00) was added. Then a scan of fluorescence intensity was performed ( $\lambda_{\text{ex}} = 450$  nm;  $\lambda_{\text{em}} = 485$  nm). The fluorescence intensities were recorded, and the percentage of inhibition on aggregation was calculated by the following expression:  $(1 - I_{\text{Fi}}/I_{\text{Fc}}) * 100\%$  in which  $I_{\text{Fi}}$  and  $I_{\text{Fc}}$  were the fluorescence intensities obtained for absorbance in the presence and absence of inhibitors, respectively, after subtracting the fluorescence of respective blanks. Each assay was performed in triplicate.

### 5.5. MTT assay of HepG2 and PC12 cell viability

MTT assay of PC12 and HepG2 was conducted according to the previous report [16].

### 5.6. Behavioral Studies

All experiments were performed in accordance with the National Institutes of Health Guide for the Care and Use of Laboratory Animals. The procedures were approved by the Animal Care and Use Committee of the Henan University. Kunming Mice, (male,  $20 \pm 2$ g) were purchased from Experimental Animal Center of Zhengzhou University (Zhengzhou, China). The mice were housed in SPF grade animal room, and kept in plastic cages in the Experimental Animal Center of Henan University (Kaifeng, China). The animals were provided with free access to food and water.

Behavioral studies were performed with adult male ICR mice (8–10 weeks old, weight 20–25 g) from Beijing Vital River Laboratory Animal Technology Co., Ltd. (Beijing, China) by MWM. The mice were divided into four groups: control (vehicle), model (scopolamine), THA (scopolamine plus THA), and **5f** (scopolamine plus compound **5f**). THA and **5f** at the dose of 20  $\mu$ mol/kg body weight per day were orally administered to the mice at 30 min before the intraperitoneal (ip) administration of scopolamine (1 mg/kg). Memory impairment was induced by administering scopolamine and the maze task was performed after 30 min of scopolamine administration. The schematic diagram (Figure

S1) depicts the experimental procedure.

MWM is a circular pool (100 cm in diameter and 50 cm in height) with visual cues. The circular pool was filled at a depth of 30 cm with water (25 °C). A platform (6 cm in diameter and 29 cm in height) was centered in one of four quadrants of the pool. Mice were trained during trial sessions of four trials each day for four consecutive days. During each trial, the mouse's escape latency was recorded. Once the mouse located the platform, it was permitted to remain on it for 10s. If the mouse did not locate the platform within 90 s, it was placed on the platform for 10s. On the fifth day after training, mice were given a probe trial session in which the platform was moved from the pool and allowing the mice to swim for 90s. The time and the distance taken in the target quadrant and the number of times the animals crossed the platform location were recorded.

## Acknowledgements

We thank the Natural Science Foundation of China (No. U1704176, 81460528, 21762010), the Foundation for University Key Teacher by Educational Commission of Henan Province (No. 2016GGJS-030), the Natural Science Foundation of Guangxi Province of China (2018GXNSFAA281135)

## Conflict of Interest

We declare that we have no conflict of interest.

## References and notes

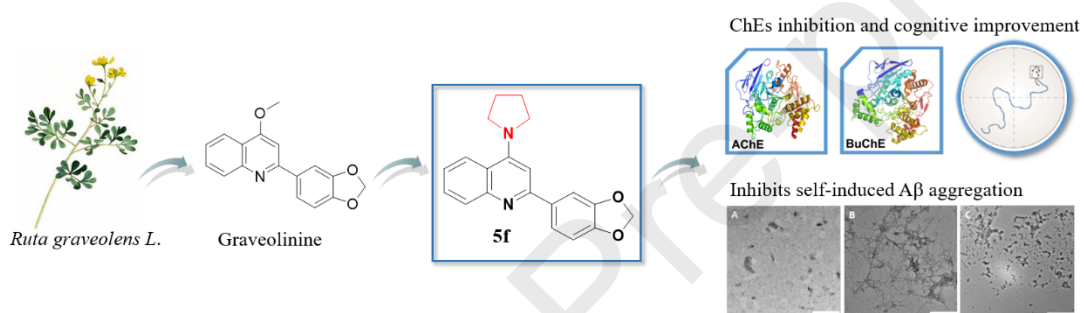
[1] Sameem, B.; Saeedi, M.; Mahdavi, M.; Shafiee, A. *Eur. J. Med. Chem.* **2017**, *128*, 332.

- [2] Chopra, K.; Misra, S.; Kuhad, A. *Expert Opin. Ther. Targets* **2011**, *15*, 535.
- [3] Huang, L.; Su, T.; Shan, W.; Luo, Z.; Sun, Y.; He, F.; Li, X. *Bioorg. Med. Chem.* **2012**, 3038.
- [4] Tundis, R.; Bonesi, M.; Menichini, F.; Loizzo, M. R. *Mini-Rev Med. Chem.* **2016**, *16*, 605.
- [5] Kamal, M. A.; Klein, P.; Luo, W.; Li, Y.; Holloway, H. W.; Tweedie, D.; Greig, N. H. *Neurochem. Res.* **2008**, *33*, 745.
- [6] Greig, N. H.; Utsuki, T.; Ingram, D. K.; Wang, Y.; Pepeu, G.; Scali, C.; Yu, Q. S.; Mamczarz, J.; Holloway, H. W.; Giordano, T.; Chen, D.; Furukawa, K.; Sambamurti, K.; Brossi, A.; Lahiri, D. K. *Proc. Natl. Acad. Sci.* **2005**, *102*, 17213.
- [7] Elsinghorst, P. W.; Tanarro, C. M.; Gutschow, M. *J. Med. Chem.* **2006**, *49*, 7540.
- [8] Oliva, A.; Meepagala, K. M.; Wedge, D. E.; Harries, D.; Hale, A. L.; Aliotta, G.; Duke, S. O. *J. Agric. Food Chem.* **2003**, *51*, 890.
- [9] Bandatmakuru, S. R.; Arava, V. R. *Synthetic Commun.* **2018**, *48*, 2635.
- [10] Wu, T. S.; Shi, L. S.; Wang, J. J.; Iou, S. C.; Chang, H. C.; Chen, Y. P.; Kuo, Y. H.; Chang, Y. L.; Tenge, C. M. *J. Chin. Chem. Soc.* **2003**, *50*, 171.
- [11] Wu, T. S.; Li, C. Y.; Leu, Y. L.; Hu, C. Q. *Phytochemistry* **1999**, *50*, 509.
- [12] Ivanova, A.; Mikhova, B.; Najdenski, H.; Tsvetkova, I.; Kostova, I. *Fitoterapia* **2005**, *76*, 344.
- [13] Li, Z.; Mu, C.; Wang, B.; Jin, J. *Molecules* **2016**, *21*, 132.
- [14] Luo, W.; Su, Y. B.; Hong, C.; Tian, R. G.; Su, L. P.; Wang, Y. Q.; Li, Y.; Yue, J. J.; Wang, C. J. *Bioorg. Med. Chem.* **2013**, *21*, 7275.
- [15] Zhang, X.; Wang, J.; Hong, C.; Luo, W.; Wang, C. J. *Acta Pharm. Sin. B* **2015**, *5*, 67.
- [16] Luo, W.; Chen, Y.; Wang, T.; Hong, C.; Chang, L. P.; Chang, C. C.; Yang, Y. C.; Xie, S. Q.; Wang, C. J. *Bioorg. Med. Chem.* **2016**, *24*, 672.

- [17] Huang, L.; Luo, Z.; He, F.; Lu, J.; Li, X. S. *Bioorg. Med. Chem.* **2010**, *18*, 4475.
- [18] Shi, A. D.; Huang, L.; Lu, C. J.; He, F.; Li, X. S. *Bioorg. Med. Chem.* **2011**, *19*, 2298.
- [19] Ellman, G. L.; Courtney, K. D.; Andres, V., Jr.; Feather-Stone, R. M. *Biochem. Pharmacol.* **1961**, *7*, 88.
- [20] Huang, L.; Shi, A.; He, F.; Li, X. *Bioorg. Med. Chem.* **2010**, *18*, 1244.
- [21] Morris, G. M.; Goodsell, D. S.; Halliday, R. S.; Huey, R.; Hart, W. E.; Belew, R. K.; Olson, A. J. *J. Comput. Chem.* **1998**, *19*, 1639.
- [22] Huang, L.; Miao, H.; Sun, Y.; Meng, F.; Li, X. S. *Eur. J. Med. Chem.* **2014**, *84*, 429.
- [23] Akrami, H.; Mirjalili, B. F.; Khoobi, M.; Nadri, H.; Moradi, A.; Sakhteman, A.; Emami, S.; Foroumadi, A.; Shafiee, A. *Eur. J. Med. Chem.* **2014**, *84*, 375.
- [24] Najafi, Z.; Mahdavi, M.; Saeedi, M.; Karimpour-Razkenari, E.; Asatouri, R.; Vafadarnejad, F.; Moghadam, F. H.; Khanavi, M.; Sharifzadeh, M.; Akbarzadeh, T. *Eur. J. Med. Chem.* **2017**, *125*, 1200.
- [25] Bartolini, M.; Bertucci, C.; Bolognesi, M. L.; Cavalli, A.; Melchiorre, C.; Andrisano, V. *Chembiochem* **2007**, *8*, 2152.

## Synthesis, in vitro and in vivo biological evaluation of novel graveolinine derivatives as potential anti-Alzheimer agents

Wen Luo <sup>§,a</sup>, Jian-Wu Lv <sup>§,a</sup>, Ting Wang <sup>a</sup>, Zhi-Yang Zhang <sup>a</sup>, Hui-Yan Guo <sup>a</sup>, Zhi-Yi Song <sup>b</sup>, Chao-Jie Wang <sup>a</sup>, Jing Ma <sup>b,\*</sup>, Yi-ping Chen <sup>c,\*</sup>



- > A novel series of graveolinine derivatives were synthesized and evaluated as potential anti-Alzheimer's agents.
- > Compound **5f** showed moderate inhibitory activities for AChE, BuChE and A $\beta$  self-aggregation.
- > Compound **5f** significantly ameliorates the cognitive performances of scopolamine-treated ICR mice.

**Declaration of interests**

The authors declare that they have no known competing financial interests or personal relationships that could have appeared to influence the work reported in this paper.

The authors declare the following financial interests/personal relationships which may be considered as potential competing interests:

Journal Pre-proofs